Mesoscopic coherence phenomena in semiconductor devices

by S. B. Kaplan
A. Hartstein

Semiconductor devices have several attractive properties which make them useful in the study of electronic coherence phenomena such as universal conductance fluctuations. The use of gated devices allows the Fermi level, and thus the electronic wavelength, to be adjusted in order to study energy correlation effects. The two-dimensional electron gas formed beneath the gate can be tilted with respect to the magnetic field to reveal that the field correlation length of the fluctuations obeys a cosine law. This strongly suggests that the fluctuations are caused by quantum interference in the same way that the Aharonov–Bohm effect arises in metallic rings. The energy range over which electrons are correlated in these materials is generally larger than in metals. This allows one to study these conductance fluctuations at much higher temperatures than are feasible in metallic conductors. For the same reason, substantially larger source–drain voltages can be applied to observe asymmetry and nonlinear effects in the conductance.

1. Introduction

Electronic transport in very small disordered conductors has been the subject of intense study in recent years. The transport properties of both small and large systems are substantially affected by electronic scattering from sites of disorder, such as crystal imperfections and impurities. Many of the more interesting properties of small conducting systems are dependent on the particular impurity configuration of each sample [1, 2]. Such sample-specific behavior is not readily apparent in transport measurements using large samples, because the dissimilar contributions of an ensemble of small regions are averaged in such measurements.

This paper is concerned with the sample-specific behavior of the "metallic" samples, in which the localization length (the spatial extent of the electronic wave function) is greater than the sample size. The conductance of samples in the metallic limit is larger than $\sim e^2/h$, which is approximately $(25\ \mathrm{k}\Omega)^{-1}$ [3]. Electronic interference plays a major role in quantum corrections to the conductance in the metallic regime [4, 5]. Interference effects can only take place between electronic states that are phase-coherent. The length scale, L_ϕ, over which phase coherence occurs is limited by phase-disturbing scattering processes. For a disordered conductor, the phase-coherence length is given by $L_\phi \equiv \sqrt{D\tau_\phi}$. L_ϕ is thus related to the diffusion constant D and the lifetime τ_ϕ, which includes all phase-breaking processes such as inelastic and spin-flip scattering. Note that *elastic* scattering does not disturb the phase [6, 7], and

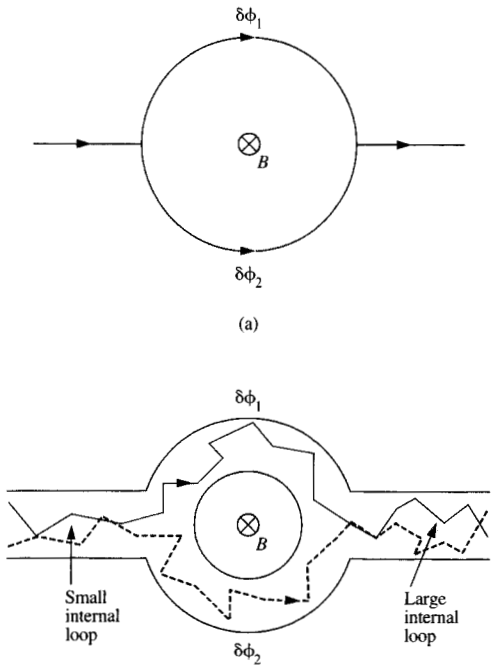

Figure 1

(a) An Aharonov–Bohm loop, in which an electron beam is split in two and rejoined. The phase difference $\delta\phi_1 - \delta\phi_2$ varies with the magnetic flux penetrating the loop, resulting in a periodically varying current. (b) A schematic diagram of a disordered metallic Aharonov–Bohm loop. The leads are assumed to extend to reservoirs in which all inelastic processes take place. Two of the possible electronic paths are shown. Two ring-like pairs of trajectories that lead to aperiodic structure are identified.

therefore only limits L_ϕ through its effect on D. In the conducting channels of Si metal-oxide-semiconductor field-effect transistors (MOSFETs), and Au wires at temperatures of ~1 K, L_ϕ is of the order of 1 μm, but may be an order of magnitude larger in GaAs/AlGaAs heterostructures.

The term "mesoscopic" [8] was coined to describe systems intermediate between the atomic and macroscopic regimes in which statistical fluctuations are important. We follow Imry [9] in applying this term to systems comparable in size to L_ϕ. It has been experimentally observed that the electronic conductance of disordered metallic conductors exhibits aperiodic fluctuations as either the magnetic field or the Fermi level is varied [10–17]. The results are consistent with the theory of universal fluctuations [2, 9, 18–25], which treats the conductance of mesoscopic samples quantum-mechanically. The theory predicts a sample-specific conductance that varies aperiodically with changes in electronic phase or wavelength.

Although these aperiodic fluctuations can be found in the conductance of disordered metallic, semimetallic, and semiconducting samples, it is shown that there are several attributes of small semiconducting systems that make them especially suited to the study of such electronic coherence phenomena. We pay particular attention to results obtained using the thin layers of electrons induced by the field effect [26] in Si MOSFETs.

2. Aperiodic conductance fluctuations

The study of aperiodic fluctuations arose from the search for *periodic* Aharonov–Bohm oscillations in the magnetic-field-dependent conductance (or *magnetoconductance*) of mesoscopic conducting rings. Both of these phenomena are now known to be due to the same type of quantum interference. The salient issues may be clearly illuminated by describing the *gedanken* (or thought) experiment of Aharonov and Bohm [27]. An electron beam propagating *in vacuo* is split into two separate paths and then rejoined, as shown in **Figure 1(a)**. The resultant electronic current measured at a point downstream from the loop can be shown to be related to the difference of the quantum-mechanical phases of the wave functions in the two branches, $\phi_1 - \phi_2$. The result of a magnetic flux Φ applied to the interior of the loop is an additional phase difference between the two branches of the loop, $\delta\phi_1 - \delta\phi_2 = (e/\hbar)\Phi = (e/\hbar)\oint \mathbf{A} \cdot d\mathbf{s}$, where $\mathbf{A}$ is the magnetic vector potential and $\mathbf{s}$ is the path that encloses the flux. This implies that the current will show an oscillatory dependence on the applied flux with period h/e, where h is Planck's constant and e is the electronic charge.

Now let us replace the vacuum paths with a disordered metallic ring to which leads have been attached, as shown in **Figure 1(b)**. It is assumed that electrons suffer only elastic scattering in the conductor. The leads extend to reservoirs to which all irreversible processes (such as *inelastic* scattering) are confined, as in Landauer's pioneering work on the quantum-mechanical resistance of disordered conductors [28, 29]. The electron energies are not shifted during elastic scattering in the ring, even though momentum relaxation occurs. It was argued [6, 7] that under these circumstances, electronic phase coherence is preserved, and h/e oscillations should still be observable.

In a real ring with circumference comparable to L_ϕ, some phase-breaking does occur. However, enough phase coherence remains to produce periodic fluctuations in the magnetoconductance. The first observation of Aharonov–Bohm oscillations in single metal loops with a magnetic flux period of h/e was made by Webb et al. [30, 31]. It provided a striking validation of the concepts of quantum coherence and transport that had been developing since the early work of [28].

The observation of periodic oscillations in thin metallic loops was not made without difficulty. (This work is discussed in detail in [5] and in other articles in this issue of the *IBM Journal of Research and Development*.) One of the

more interesting aspects of the early work on single rings was the unexpected observation by Umbach et al. [10] and Blonder [11] of sample-specific aperiodic magnetoconductance fluctuations which almost completely obscured the periodic structure.

It is now believed that such aperiodic fluctuations have long been observed in experiments on small structures, but remained unexplained. A representative example is the observation of fluctuations in the conductance of narrow Si MOSFETs [32] by A. Fowler et al. The main focus of the experiment was to study the transition from one- to two-dimensional conduction in a variable-width electron accumulation layer as the gate voltage was varied. However, their data (see **Figure 2**) show significant aperiodic fluctuations. At the lower values of gate voltage, the localization (or decay) length of the electronic wave function was found to be much shorter than the phase-coherence length, indicating that the electrons were strongly localized. The fluctuations in this regime were identified with changes in the variable-range hopping paths as the Fermi level was varied [33]. The data also show that at the highest values of gate voltage, aperiodic conductance fluctuations extended into the metallic or weakly localized regime, where the localization length is longer than L_ϕ.

Y. Imry* suggested that the aperiodic magnetoconductance fluctuations in the weakly localized regime may be due to the same type of quantum interference that gives rise to the Aharonov–Bohm effect. This can be explained by noting that the electronic trajectories within the conductor actually constitute a large number of Aharonov–Bohm loops. Two such loops are pointed out in Figure 1(b). Since the magnetic field penetrates these loops, one obtains fluctuations with periodicities that reflect their respective areas. The total conductance represents the contribution from all trajectories, and is therefore aperiodic.

Imry's ideas stimulated Stone [18] to do computer simulations of a disordered conductor using the multichannel Landauer conductance formula [28, 34, 35]. The results of these simulations contained aperiodic magnetoconductance fluctuations comparable to the experimental observations of [10]. The density of the fluctuations as a function of magnetic field was found to be proportional to the area of the sample. It was concluded that this phenomenon is indeed due to the Aharonov–Bohm effect.

Simultaneous independent work was done by Al'tshuler [2], who used a weak-scattering diagrammatic technique to predict that sample-to-sample conductance fluctuations may arise because of the sample-specific interference conditions. In other words, mesoscopic conductors that are macroscopically identical, but have different impurity

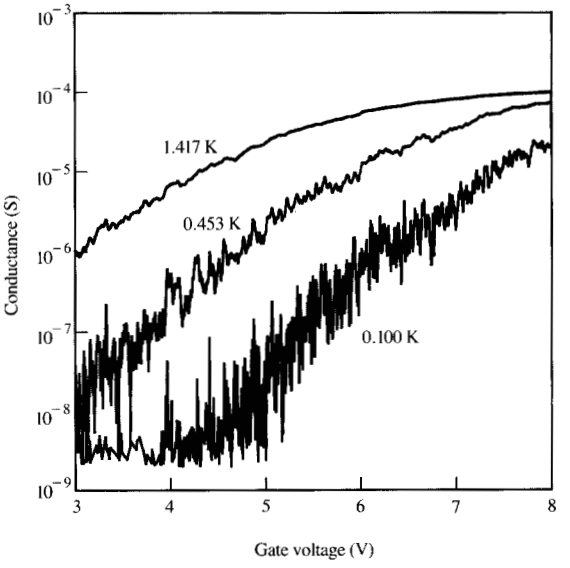

Figure 2

The conductance of a narrow Si MOSFET accumulation layer. The data show fluctuations as the gate voltage is varied. These fluctuations persist into the regime of weak localization [32].

configurations, may have different conductances. The connection between the approaches taken by Stone and Al'tshuler is clear in the work of Lee and Stone [19], wherein the hypothesis is proposed that variation of the magnetic field is identical to changing the sample.

The calculations of [19] and subsequent work [9, 20–24] made use of scattering diagrams similar to that used in [2]. These calculations are applicable to weakly localized samples in which there is sufficient elastic scattering in a sample of length $L \sim L_\phi$ that the elastic mean free path $\ell \ll L$. Fluctuations in the conductance G at magnetic field B and Fermi energy E_F were studied by calculating the conductance autocorrelation function $F(\Delta B, \Delta E) \equiv \langle G(B + \Delta B, E_F + \Delta E)G(B, E_F)\rangle - \langle G(B, E_F)\rangle^2$. Several universal properties of the conductance fluctuations were discovered:

1. The root-mean-squared (rms) fluctuation amplitude δG at $T = 0$ is given by $\delta G \equiv \sqrt{F(0, 0)}$, which is of the order of $e^2/h \equiv G_0$.
2. The same results obtain whether the sample is a metal, a semiconducting inversion layer, or an accumulation layer.
3. The fluctuation amplitude is essentially the same (to within a factor of $\sqrt{2}$ [21]), whether the electron energy or the applied magnetic field is varied.

* Y. Imry. Department of Nuclear Physics, The Weizmann Institute of Science, Rehovot 76100, Israel; private communication, 1985.

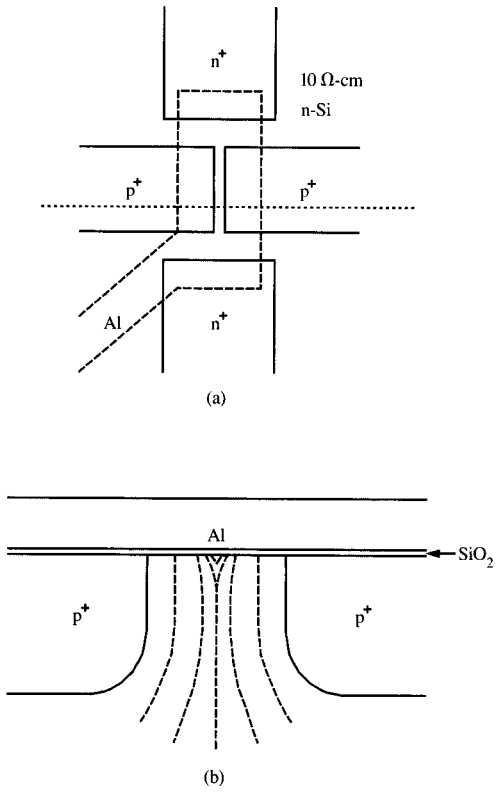

Figure 3

(a) The layout of a narrow Si accumulation layer device used in [13, 14, 32] is shown. The two p^+ control electrodes define the channel. The width between the controls is approximately 1 μm. The length of the narrow region is approximately 10 μm. The two n^+ regions are the source and drain. A cross section taken along the dotted line is shown in (b). The diffusions are about 0.5 μm deep and the oxide is 30 nm thick.

A few comments about these properties are warranted.

The prediction of a universal conductance fluctuation amplitude that is insensitive to the degree of disorder or the shape of the sample [2, 18, 19] is a remarkable statement, but it is now understood to be applicable for samples comparable in size to L_ϕ. The present formulation of the theory recognizes that samples either much larger or much smaller than L_ϕ may exhibit fluctuations substantially different from G_0 in magnitude. Samples much larger than L_ϕ sustain a large quantity of phase-breaking processes, and thus cannot be expected to exhibit as strong interference effects as smaller samples [9, 20, 21]. The coherence of voltage measurements in samples much shorter than L_ϕ leads to length-independent voltage fluctuations, resulting in conductance fluctuation amplitudes that increase with decreasing sample length [16, 23–25]. However, for a sample of size $\sim L_\phi$, the fluctuation amplitude is expected to be of the order of G_0 for a Si accumulation layer, a semimetallic Sb thin film, or a Au wire, despite the obvious differences between these materials.

One may observe fluctuations by measuring many samples, or by varying the interference conditions in a single sample [19]. In a magnetoconductance measurement, the electronic phase is varied as in the Aharonov–Bohm effect. The magnetic field autocorrelation function $F(B)$ for a two-dimensional sample larger than L_ϕ was predicted to have a width at half maximum of the order of h/eL_ϕ^2 [19]. However, if such a sample is tilted with respect to the magnetic field, only the autocorrelation function of the *perpendicular* field component should be constant.

Another way to vary the interference conditions is to vary the Fermi energy. This should result in a fluctuation in the conductance each time another wavelength is added to the path length. A simple calculation [36] shows that this happens when the energy changes by $E_\phi \sim hD/L_\phi^2$. This is approximately the width of the energy autocorrelation function $F(0, E)$ obtained by Lee and Stone [19].

The temperature scale over which the fluctuations may be observed is determined by E_ϕ. Electronic states are correlated within bands of width E_ϕ. Stone [18] has argued that when the thermal energy $k_B T$ is much greater than E_ϕ, the fluctuation patterns of a large number of uncorrelated energy bands, given by $k_B T/E_\phi$, are averaged. The fluctuation amplitude is therefore reduced by the statistical factor $\sqrt{k_B T/E_\phi}$. This slow decrease in the fluctuation amplitude with temperature allows the fluctuations to be easily observed at ^{3}He temperatures ($T > 0.3$ K) for most mesoscopic samples.

3. Measurements of universal conductance fluctuations

The experimental testing of this theoretical framework was undertaken by several groups that employed Si MOSFETs [12–15]. There are a number of differences between these devices and metallic samples that make them a practical choice for the study of mesoscopic effects. The coherence energies in MOSFETs are about an order of magnitude larger than in metals such as Au or AuPd. This arises from the differences in carrier densities between these two types of systems. (The maximum induced carrier density in a Si MOSFET is of the order of 10^{19} cm^{-3}, while a typical density in a metal is of the order of 10^{23} cm^{-3}.) This leads to relatively poorer electronic screening in MOSFETs, which in turn causes the electron–electron scattering rate in these devices to be larger than in metallic systems. As it turns out, this is the scattering process that limits τ_ϕ at low temperatures [37]. Instead of having to work at temperatures below 0.1 K, as did Umbach et al., workers studying Si

MOSFETs may work at temperatures greater than ~0.5 K. Despite the longer phase-breaking lifetime, the Fermi velocity in Si MOSFETs is correspondingly smaller, resulting in a phase-coherence length $L_\phi \sim 1$ μm at 0.5 K.

Another more fundamental difference between metallic lines and gated MOSFETs was also exploited. The Fermi level can easily be varied by adjusting the gate voltage V_G. This technique was used by Licini et al. [12] to illustrate the coherent nature of the fluctuations by measuring the magnetoconductance at various values of V_G. The fluctuations in the magnetoconductance were observed to be similar for closely spaced values of gate voltage, but were strikingly different when the gate voltage exceeded the coherence energy. This distinguished the underlying mechanism for the fluctuations from those that rely on a shift of energy levels to produce aperiodic structure. However, a definitive exhibition of the orbital nature of the important interference effects was lacking.

If the magnetoconductance fluctuations are due to the Aharonov–Bohm effect, the fluctuations should depend on the amount of magnetic flux threading the sample. In order to test this hypothesis, Kaplan and Hartstein [13, 14] exploited the two-dimensional properties of the electron gas in Si MOSFETs operated at low temperatures [38]. The electronic trajectories in such a system are essentially planar, even when the magnetic field is tilted with respect to the sample. A two-dimensional accumulation layer was tilted in a magnetic field to determine whether the perpendicular component of magnetic field is the important parameter. The samples chosen for this work were used in [32] for the study of one- and two-dimensional transport, as described in Section 2. These samples showed fluctuations in the conductance not only as the gate voltage was varied (see Figure 2), but also as the magnetic field was varied. The magnetoconductance of these devices was measured for gate voltages of 10 to 12 V. The conductance in this gate-voltage range is of the order of 10^{-4} S, which is in the metallic regime addressed by the universal fluctuation theory for $T \sim 0.5$ K.

The device layout is shown in **Figure 3(a)**. As the gate voltage is increased above the device threshold voltage, a narrow conducting channel is formed in n-type Si between the depletion region of two p^+ control electrodes. (These electrodes were shorted to the substrate during this experiment.) A side view is shown in **Figure 3(b)**. The channel length, L, is approximately 10 μm. The width of the narrow accumulation layer, W, varies with the gate voltage and cannot be measured microscopically. W was estimated to be of the order of 100 nm at $V_G = 11$ V for the most studied sample, as described later in this section.

The magnetic field, B, was varied between 0 and 1.5 T, and was oriented perpendicular to the channel. The angle θ between the vector normal to the sample surface and the magnetic field was varied by tilting the sample with a gear

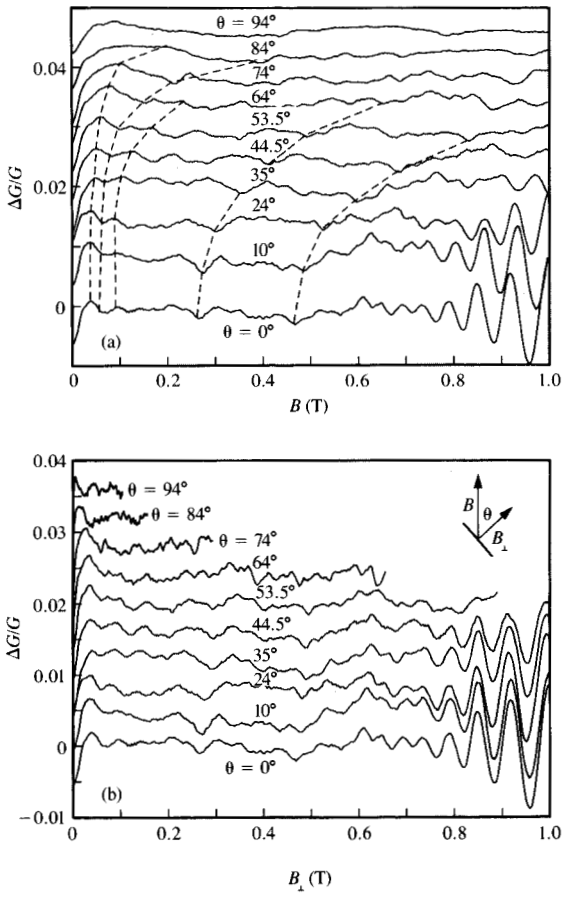

Figure 4

(a) Fractional change in the magnetoconductance of a pinched Si accumulation layer sample for various values of the angle θ between the magnetic field axis and the vector normal to the sample surface [13]. A slowly varying background has been subtracted. $V_G = 11$ V and $T = 0.47\,\text{K} \pm 0.02\,\text{K}$. $G \sim 2.3 \times 10^{-4}$ at $B = 0$. The dotted lines are used to track several structures from curve to curve as θ is varied. (b) The same data plotted vs. the perpendicular component of the magnetic field.

set. The magnetoconductance data are shown in **Figure 4(a)** for various tilt angles. (A slowly varying background and part of the low-field magnetoconductance have been subtracted.)

The two-dimensional nature of the accumulation layer is evident in the presence of the large oscillations at the largest magnetic fields, which are found to be periodic in $(B \cos\theta)^{-1}$. These Shubnikov–de Haas oscillations arise from the quantizing effect of a magnetic field [38]. The correct quantum-mechanical treatment of cyclotron motion in a magnetic field results in a set of energy levels separated in

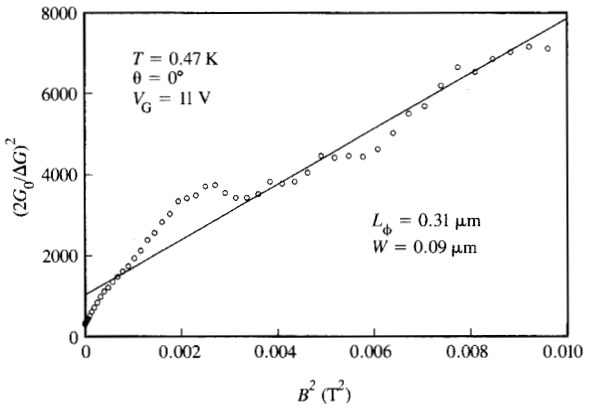

Figure 5

Inverse square of ΔG, the deviation of the magnetoconductance of a pinched Si accumulation layer from its saturation value, plotted against the square of the applied magnetic field [13]. The straight line is the best fit to the data.

energy by an amount proportional to the cyclotron frequency. Since the cyclotron frequency is linear in the magnetic field, the density of these Landau levels on the energy axis varies as B^{-1}. The electronic density of states contains peaks at the center of each of the Landau levels. The channel conductance is affected by the change in the number of electrons contributing to the transport as the magnetic field causes these levels to move through the Fermi level. The confinement of the electronic trajectories to two dimensions causes the Landau levels to be spaced proportional to the perpendicular component of the applied field, allowing an independent check of the tilt angle.

The aperiodic fluctuations in the magnetoconductance data are easily seen in Figure 4(a). The peaks and dips are observed to appear at larger values of B as the tilt angle increases. The data are replotted vs. the perpendicular component of the applied field in **Figure 4(b)**. One can see that the fluctuations lie at nearly the same value along the abscissa. This shows that the dominant contribution to the fluctuations is orbital in nature, as is expected for Aharonov–Bohm interference. Similar effects have subsequently been observed using GaAs samples [39, 40]. The data of [40] clearly show the $B \cos \theta$ dependence of the fluctuations.

It was observed in [12–14] that the measured fluctuation amplitudes were much smaller than G_0. At first, this appeared to disagree with the universal fluctuation theory, but the prediction of a universal fluctuation amplitude is predicated on the assumption that phase-breaking processes are unimportant. This is certainly not true when the sample size exceeds L_ϕ. Each coherent subsection of the sample has conductance fluctuations of the order of G_0. Theoretical calculations show that the fluctuation amplitude for a large sample is equivalent to the contribution of a classical series-parallel network of resistors, each resistor representing a subsection of size $\sim L_\phi$ [9, 20, 21]. This results in an rms amplitude that may be substantially less than G_0. In order to reconcile theory and observation, the sample dimensions must be compared with the phase-coherence length. The experimental determination of L_ϕ is a rather difficult business. We discuss the method used in [13, 14] to estimate L_ϕ, and include some more recent experimental observations to verify the accuracy of that estimate.

It is fortuitous that electron coherence is important in the theory of weak localization [4], because it presents an opportunity to estimate L_ϕ. The weak localization of electrons in disordered metals arises from the coherent backscattering of time-reversed pairs of electrons. This backscattering decreases the conductance by an amount of the order of e^2/h. A perpendicular magnetic field changes the phase of these electronic pairs and destroys the phase-coherent localization process. As a result, there is a negative magnetoresistance [41]. All coherent trajectories must be taken into account; phase-breaking processes are important for trajectories longer than L_ϕ. For samples of width $W < L_\phi$, the areas of the largest coherent trajectories are also limited by W. This turns out to be the appropriate limit for the pinched accumulation-layer samples. The dephasing for such a narrow sample occurs on a magnetic field scale such that the flux through an area WL_ϕ is of the order of the flux quantum h/e. For narrow samples in which spin-flip scattering is negligible, the correction to the conductance due to weak localization $\Delta G = G(B \to \infty) - G(B = 0)$ is given by [42]

$$\left(\frac{2G_0}{\Delta G}\right)^2 = L^2\left\{L_\phi^{-2} + \left(\frac{e}{\hbar}\right)^2 \frac{W^2B^2}{3}\right\}. \quad (1)$$

A typical set of data for $V_G = 11$ V and $\theta = 0°$ is shown in **Figure 5**. We plot $(2G_0/\Delta G)^2$ versus B^2 to compare directly to Equation (1). The presence of conductance fluctuations produces deviations from the fit. The best fit to the data results in estimates of $L_\phi \sim 0.3 \pm 0.1$ μm and $W \sim 0.1 \pm 0.03$ μm.

The presence of strong fluctuations makes it difficult to fit the data using Equation (1) in order to find L_ϕ and W. To check the veracity of our estimates of W and L_ϕ, low-field magnetoconductance curves were obtained (using a different sample) by varying V_G from 10 to 12 V in steps of 0.25 V. The conductance of the sample varied by only ~25 percent within this gate-voltage range. Each step corresponded to changing the Fermi level by $\sim E_\phi$. Each data set therefore had a different fluctuation pattern, and conceptually represented a different sample [19]. By analyzing each individual curve, it was found that W typically ranged from 0.08–0.09 μm.

L_ϕ varied from 0.46 to 0.60 μm. An average magnetoconductance (see **Figure 6**) was calculated by averaging the conductance values of all data sets at the same value of magnetic field. The fluctuation amplitude is drastically reduced, which graphically shows the effects of averaging many different samples. The analysis shows $W \sim 0.08 \pm 0.01$ μm and $L_\phi \sim 0.5 \pm 0.1$ μm. These data were used in estimating the error bars for L_ϕ and W quoted for the sample used in the tilted-field experiment. We can now use these data to estimate the expected reduction in fluctuation amplitude due to size effects.

The length and width of the narrow accumulation layer at $V_G = 11$ V are found to obey the inequality $W < L_\phi \ll L$. Therefore, the fluctuation amplitude is calculated by averaging the contribution of a series string of $N = L/L_\phi$ resistors, each of which fluctuates with an amplitude of $\sim G_0$ [9, 21]. The resistance of the string is the sum of the separate fluctuating resistances. The rms fluctuation amplitude of the *total resistance* is found by using the central limit theorem [43] to be $\sqrt{N}$ times the fluctuation amplitude of the resistors in the string, δr. This result may be rewritten in terms of the conductance fluctuation of the string, $\delta G = \delta(1/R)$, and the conductance fluctuation of one of the resistors, $\delta g = \delta(1/r) = G_0$. The theoretical calculations for a sample in the limit $W < L_\phi \ll L$ predict the rms magnetoconductance fluctuation amplitude for the entire sample to be [9, 21]

$$\delta G_{\text{rms}} \sim (L_\phi/L)^{3/2} G_0, \qquad (2)$$

which results in a predicted fluctuation amplitude of $2.2 \pm 0.5 \times 10^{-7}$ S, in reasonable agreement with the measured value of $2 \pm 0.5 \times 10^{-7}$ S at a temperature $T = 0.5$ K.

It should be mentioned that many of the measurements of fluctuations in [12] were taken at temperatures exceeding E_ϕ/k_B. Therefore, a number equal to $k_B T/E_\phi$ energy bands of width E_ϕ contribute to the fluctuations. As mentioned earlier, the fluctuation amplitude is therefore reduced by the statistical factor $\sqrt{k_B T/E_\phi}$ [18, 19, 44], in addition to the reduction due to size effects [9, 20, 21].

The size dependence of the fluctuation amplitude in the low-temperature limit where $k_B T \ll E_\phi$ has now been studied in considerable detail, using narrow Si inversion layers [15, 17] as well as metal wires [16]. The initial conclusions of this work [15] claimed consistency (within a factor of ~2) with Equation (2) for narrow samples. In subsequent work, voltage fluctuations were found to become length-independent for probes spaced closer than L_ϕ [16, 17], resulting in a fluctuation amplitude which increases as L^{-2}. This effect is due to the fact that the interference of electrons that diffuse into voltage probes can substantially affect voltage measurements. In other words, the measurement of voltage is inherently nonlocal on a mesoscopic scale.

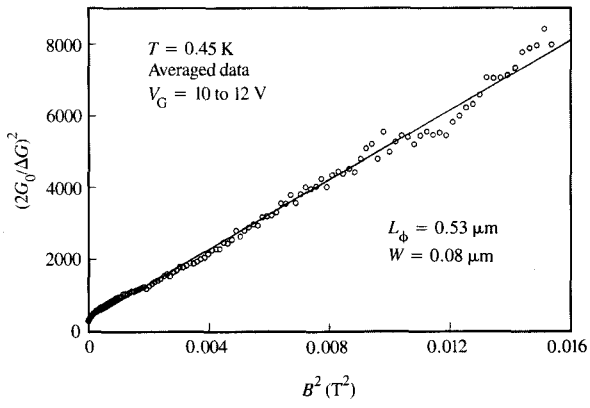

Figure 6

A plot of the low-field magnetoconductance of a pinched Si accumulation layer similar to that of Figure 5, but using a different sample. The inverse square of the average of many data sets for ΔG is plotted versus B^2. These data are nearly linear, and show a reduced fluctuation amplitude. The values of W and L_ϕ obtained by the best fit to the data are similar to those obtained from each of the separate data sets, which contain significant fluctuations.

It is now well established that fluctuations in disordered conductors are caused by interference effects. The conductance fluctuation theory in its present form describes the magnetic field, energy, and size dependences very well, in the sense that error bars overlap or lie close to theoretical predictions. Si MOSFETs played an important role in determining the underlying mechanism, and in the study of size effects. However, this discussion would not be complete without mentioning some new developments involving other semiconducting devices.

Several experimental groups are now measuring fluctuations in small GaAs/AlGaAs heterostructures. Magnetoconductance oscillations attributed to the Aharonov–Bohm effect have been observed in a coupled double-layer heterostructure [45]. Other experiments are being performed on GaAs-based heterostructure samples that have probe spacings of the order of the mean free path, ℓ, which may be as large as 5 or 6 μm [46–48]. The width of some of these samples is of the same order as the electronic wavelength. The presence of only a small amount of disorder in these conductors, and their quasi-one-dimensional nature, places them outside the realm of the universal fluctuation theory. Indeed, it is one that is theoretically difficult to treat. Aperiodic fluctuations have been observed in the diagonal and off-diagonal (Hall) resistances, corresponding to a fluctuation amplitude of up to $80G_0$. The fluctuations reported in [46] represent a large enough fraction of the

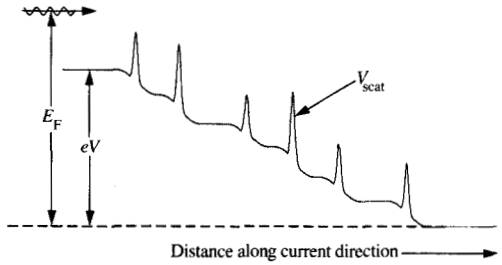

Figure 7

A schematic energy diagram for a disordered metallic sample under a voltage bias V (from [50]). The net current is toward the right. Electrons of energy E_F scatter from the random potential V_{scat}. If the bias is large enough, the wavelength of an electron may be substantially shifted.

sample resistance (5 to 10 percent) that negative dynamic resistance was observed. Aperiodic fluctuations were observed at magnetic fields up to 12 T in these mesoscopic rings. Aharonov–Bohm oscillations with amplitude of the order of G_0 have also been seen, but the fluctuation amplitude was suppressed when the cyclotron radii reached a magnitude of the order of half the device linewidth. These observations are not yet understood. However, with the use of these samples, the possibility exists for studying the nature of coherence effects on a length scale of ℓ.

It is clear that there is a wealth of physical phenomena to be studied, and that the development of samples with long coherence lengths and novel device structures may open new avenues of research. In contrast, the experiment described in the next section was done using a device that was designed for technological purposes. It reminds us that interesting phenomena are waiting to be uncovered in the most conventional devices.

4. Asymmetric conductance and nonlinear effects

The random placement of scatterers in a disordered conductor presents an opportunity to observe novel sample-specific mesoscopic effects. It has been predicted that the interference conditions in a conductor vary with the voltage imposed across it, thus producing a nonlinear and asymmetric conductance [20]. For example, when a source–drain bias is applied to a Si MOSFET, the disordered scattering potential becomes tilted by the bias energy eV (see **Figure 7**). The excess energy, $E_F - V_{scat}$, determines the electronic wavelength. These energies are randomly distributed, because of the disordered nature of the potential. When the random potential is tilted, the wavelengths, and therefore the phase shifts, are changed [49]. A significant (but random) total phase change is possible along a coherent electronic trajectory when the voltage across it exceeds E_ϕ/e. The variation of interference conditions with source–drain bias leads to a nonlinear conductance. When the bias is reversed, the interference conditions are substantially different than for the original bias polarity, because disordered samples lack inversion symmetry with respect to exchange of source and drain. This leads to an asymmetric conductance.

In order to observe these effects, Kaplan has measured the dependence of the conductance of Si MOSFETs with submicron dimensions as a function of the source–drain voltage, V_{SD} [50]. These devices were fabricated using a polysilicon gate and a self-aligned source and drain. The conductance of one such device, with $L \sim 0.9$ μm and $W \sim 0.5$ μm, was first studied using $V_{SD} = 5$ μV. This value of source–drain voltage is much less than either E_ϕ or $k_B T$, thus ensuring that heating and nonlinear effects are negligible. The magnetoconductance fluctuations of this device were measured in order to estimate the important parameters L_ϕ and $E_\phi \sim hD/L_\phi^2$. The gate-voltage range over which the magnetoconductance fluctuations are correlated corresponded to a change in the Fermi level by 0.2 ± 0.1 meV. This should be roughly equal to E_ϕ. One can estimate L_ϕ by comparing the measured fluctuation amplitude ($\delta G \sim 9 \times 10^{-6}$ S) to the amplitude expected for the series-parallel combination of (L/L_ϕ) by (W/L_ϕ) resistors, using the two-dimensional analogue of Equation (2) [9, 20, 21]. This resulted in a calculated E_ϕ of 0.75 meV, which is much too large. It turns out that this device is not much larger than L_ϕ. Each coherent sample region of area $\sim L_\phi^2$ is subject to different boundary conditions. In order to avoid difficulties associated with boundary effects in such a small sample [51], the fluctuations in this device were compared with the fluctuations in a larger device, with $L = 2.3$ μm and $W = 3.1$ μm, in order to determine E_ϕ.

The coherence length L_ϕ of the larger MOSFET was estimated to be ~ 0.3 μm by measuring the fluctuation amplitude ($\delta G \sim 3.6 \times 10^{-6}$ S) and then using the analogue of Equation (2) for a two-dimensional sample [9, 20, 21]. The fluctuations in the smaller device were too large to use the two-dimensional analogue of the weak-localization formula Equation (1) to estimate L_ϕ. Alternatively, L_ϕ was estimated by observing the density of the magnetoconductance fluctuations for the smaller device (or, to be more precise, the width of the magnetic-field correlation function), and comparing it to that for the larger device. The average change in magnetic field between fluctuation peaks is related to the average area of a coherent trajectory. That is, the width of the magnetic-field correlation function (at half maximum) for a two-dimensional sample with L, $W > L_\phi$ in the low-temperature

limit is given by $B_C \propto \Phi_0/L_\phi^2$ [21, 52]. The autocorrelation function calculated for both large and small devices had widths $B_C \sim 0.12 \pm 0.2$ T, indicating that the samples had identical phase-coherence lengths. L_ϕ is therefore estimated to be 0.3 ± 0.15 μm for the small device. E_ϕ was estimated to be ~0.17 meV. This is in good agreement with the value of ~0.2 meV by observing the gate-voltage range over which the magnetoconductance fluctuations are correlated. One then expects to observe nonlinear effects when the voltage across a coherent length of sample is of the order of 0.2 mV, or when $V_{SD} \sim 0.3$ to 0.6 mV.

When the source–drain voltage V_{SD} was increased, the conductance was observed to become nonlinear and asymmetric. The shape of the conductance-voltage characteristic varied aperiodically with the applied magnetic field, providing a first indication that this is an interference effect. The data for the antisymmetric magnetoconductance $G_A \equiv [G(V_{SD}) - G(-V_{SD})]$ are shown in **Figure 8**. The magnetoconductance fluctuation patterns are shown to be similar to one another until V_{SD} approaches ~0.3 meV. Since V_{SD} is distributed over approximately three lengths of L_ϕ, this corresponds to a coherence energy of ~0.1 meV, which indicates that the coherence properties of the asymmetric fluctuation patterns are similar to those of the fluctuations observed at low source–drain voltage.

The magnitudes of the antisymmetric magnetoconductance fluctuations shown in Figure 8 increase with V_{SD}. This is as one would expect, since the asymmetry of the dephasing processes becomes more pronounced as the potential becomes more tilted. For a conductor with maximum dimension of the order of L_ϕ, the low-temperature limit of the antisymmetric fluctuation amplitude is predicted by Al'tshuler and Khmel'nitskii to be [20]

$$\delta G_A \equiv \langle [G(V) - G(-V)]^2 \rangle^{1/2} \sim G_0 \times (eV_{SD}/E_\phi). \qquad (3)$$

The fluctuations in a device larger than L_ϕ must decrease due to the averaging of the contributions of coherent-device subregions [53], in a way similar to that discussed for the small-voltage fluctuations. Furthermore, there are some other complications in a real experiment when the voltage across a length L_ϕ, $eV_{SD}L_\phi/L$, approaches E_ϕ. Electron scattering results in a higher electron temperature. This temperature may be of the order of 3 or 4 K at some of the largest values of V_{SD} used in this experiment. L_ϕ decreases with increasing temperature, changing the number of coherent-sample subregions and thus decreasing the fluctuation amplitude. It is therefore not possible to vary V_{SD} without causing other changes. The averaging of different coherent energy bands must also become important when $k_B T$ exceeds E_ϕ. An attempt was made to separate these parasitic effects (at least partially) from the asymmetric behavior under study by comparing G_A to the symmetric amplitude $G_S \equiv [G(V_{SD}) + G(-V_{SD})]$, which is also affected by heating effects.

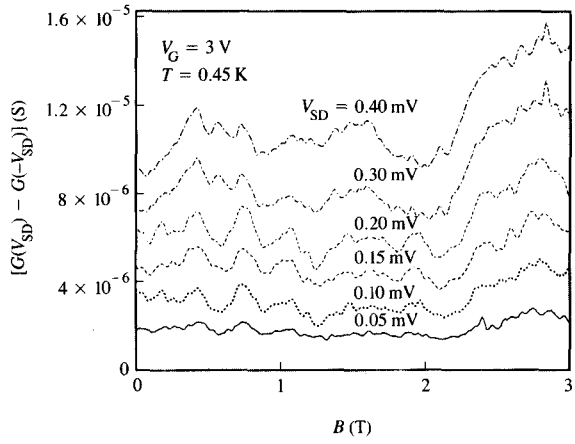

Figure 8

The fluctuations in the antisymmetric magnetoconductance for several values of source–drain voltage V_{SD} [50]. Each curve has been arbitrarily displaced along the vertical scale. Note that the patterns change shape when V_{SD} changes by more than 0.2 mV.

Both G_A and G_S are plotted in **Figure 9(a)**. The decrease in the symmetric fluctuation amplitude with V_{SD} graphically shows the effects of electron heating. G_A increases rather linearly with V_{SD} until $V_{SD} \sim 0.3$ mV, then decreases. This decrease is most likely due to the same cause as the decrease of G_S. The ratio $\delta G_A/\delta G_S$ is plotted in **Figure 9(b)**. This gives a rough idea of how G_A behaves in the absence of electron heating. We see that there is a linear increase up to $V_{SD} \sim 0.3$ mV, followed by a sublinear increase. The fact that the change in slope occurs near where $\delta G_A = \delta G_S$, and at the same value of V_{SD} that causes a change in the fluctuation pattern, lends support to the argument that this effect is due to quantum interference, and is the effect predicted in [20].

The change of the ratio $\delta G_A/\delta G_S$ in Figure 9(b) to a nonlinear slope occurs when $eV_{SD} > E_\phi$. This behavior is explained in [53]. The number of coherent energy levels spanned by the source–drain voltage is given by $N = eV_{SD}/E_\phi$. Each of these levels contributes randomly to the conductance, resulting in an $\sqrt{N}$ dependence of the fluctuation amplitude. (This result is similar to that obtained by adding N incoherent conductors in parallel.) A more detailed reconciliation between theory and experiment is not easily performed, because G_S also depends somewhat on V_{SD} [54]. Heating effects can be alleviated in shorter samples, where electrons may traverse the sample without scattering inelastically. Such work is being carried out. In fact, careful measurements on a range of channel lengths may reveal some of the details of nonequilibrium effects in short MOSFETs.

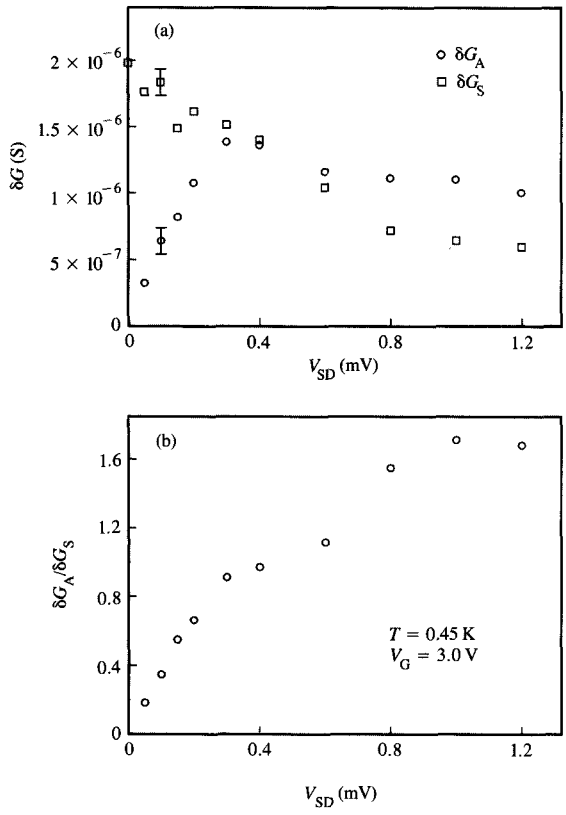

Figure 9

(a) The rms amplitudes of the antisymmetric (δG_A) and the symmetric (δG_S) components of the conductance are plotted vs. V_{SD} [50]. The symmetric fluctuation amplitude decreases with source–drain voltage. The asymmetric amplitude increases up to $V_{SD} \sim 0.3$ mV, then decreases. (b) The ratio $\delta G_A/\delta G_S$ is plotted vs. V_{SD}. The data increase linearly up to $V_{SD} \sim 0.2$ mV. Beyond this point, the increase is sublinear.

5. Conclusions

Mesoscopic effects have been studied in several types of samples: metallic and semimetallic rings and lines as well as semiconducting devices. The universality of mesoscopic interference effects is exemplified by its ubiquity in small weakly localized samples without regard to shape or material. The fabrication of gated semiconductor devices may be more complicated than that of metal lines, but it has been shown here that there are distinct advantages to their use in studying mesoscopic effects, such as the ability to carry out experiments at temperatures above 0.5 K.

Si MOSFETs were used to observe that aperiodic magnetostructure in the weakly localized regime is correlated over a certain energy scale. Experiments were performed with samples tilted with respect to the magnetic field. The results showed that the fluctuations correlated with the perpendicular component of the magnetic field, not with the total field strength. Further work revealed the dependence of the fluctuation amplitude on the sample size. These observations, together with those made on metallic and semimetallic samples, form a strong empirical framework on the theoretical foundation of universal conductance fluctuations: Quantum interference in disordered conductors leads to sample-specific fluctuations in the device transport properties.

It has also been shown that the lack of inversion symmetry in mesoscopic samples leads to nonlinear and asymmetric conductances, as made manifest by quantum interference. Second-harmonic generation and rectification are thus possible. In the absence of electron heating, these effects should increase with the voltage across the sample. In real devices, electron heating does take place, but heating does not totally obscure the asymmetry or the fluctuations. This relative insensitivity to temperature is a striking property of mesoscopic coherence effects.

There are several new directions being taken by experimentalists in the study of mesoscopic phenomena. The fabrication of near-ballistic samples, in which the spacing of voltage probes can be made shorter than the electronic mean-free path, is resulting in a wealth of novel observations. However, much work remains to be done. Another direction which is being taken is toward more strongly localized samples. Fluctuations have been observed below the mobility edge of long [55] and short samples [56]. There is current interest in the experimental study of fluctuation behavior in the transition region between weak and strong localization [9, 14, 57]. Experimental work on this subject is in progress.

One can see that there has been a wide range of experiments, with many unexplored avenues and approaches. Semiconductor devices are sure to play an important role in the continuing discovery of novel mesoscopic phenomena.

Acknowledgments

The authors are grateful to M. Büttiker, Y. Imry, R. Landauer, P. A. Lee, P. Santhanum, and A. Williams for interesting discussions. One of us (S.B.K.) would like to thank J. Sun for providing samples. The technical assistance of N. Albert and J. Tornello is also acknowledged.

References and notes

1. M. Ya. Azbel, "Resonance Tunneling and Localization Spectroscopy," *Solid State Commun.* **45,** 527–530 (1983).
2. B. L. Al'tshuler, "Fluctuations in the Extrinsic Conductivity of Disordered Conductors," *Pis'ma Zh. Eskp. Teor. Fiz.* **41,** 530–533 (1985) [*JETP Lett.* **41,** 648–651 (1985)].
3. D. J. Thouless, "Maximum Metallic Resistance in Thin Wires," *Phys. Rev. Lett.* **39,** 1167–1170 (1972).
4. For a review of coherence effects relating to weak localization, see G. Bergmann, "Weak Localization in Thin Films—A

Time-of-Flight Experiment with Conduction Electrons," *Phys. Rep.* **107,** 1–57 (1984).
5. For a review of interference effects in small conducting systems, see S. Washburn and R. A. Webb, "Aharonov–Bohm Effect in Normal Metal—Quantum Coherence and Transport," *Adv. Phys.* **35,** 375–422 (1986) or other articles in this issue of *IBM J. Res. Develop.*
6. L. Gunther and Y. Imry, "Flux Quantization Without Off-Diagonal Long Range Order in a Thin Hollow Cylinder," *Solid State Commun.* **7,** 1391–1394 (1969).
7. M. Büttiker, Y. Imry, and R. Landauer, "Josephson Behavior in Small Normal One-Dimensional Rings," *Phys. Lett.* **96A,** 365–367 (1983).
8. N. G. van Kampen, in *Statistical Physics, Proceedings of the IUPAP International Conference*, L. Pál and P. Szápfalusy, Eds., North-Holland Publishing Co., Amsterdam, 1976, p. 31 *ff*; N. G. van Kampen, "The Expansion of the Master Equation," *Advances in Chemical Physics*, I. Prigogine and S. A. Rice, Eds., John Wiley & Sons, Inc., New York, 1976, pp. 245–309.
9. Y. Imry, "Active Transmission Channels and Universal Conductance Fluctuations," *Europhys. Lett.* **1,** 249–256 (1986).
10. C. P. Umbach, S. Washburn, R. B. Laibowitz, and R. A. Webb, "Magnetoresistance of Small, Quasi-One-Dimensional, Normal Metal Rings and Lines," *Phys. Rev. B* **30,** 4048–4051 (1984); R. A. Webb, S. Washburn, C. P. Umbach, and R. B. Laibowitz, "Aperiodic Structure in the Magnetoresistance of Very Narrow Metal Rings and Lines," *Localization, Interaction and Transport Phenomena in Impure Metals*, B. Kramer, G. Bergmann, and Y. Bruynseraede, Eds., Springer-Verlag, New York, 1985, pp. 121–129.
11. G. Blonder, "Flux Quantization in GaAs Rings at Low Temperatures," *Bull. Amer. Phys. Soc.* **29,** 535 (1984).
12. J. C. Licini, D. J. Bishop, M. A. Kastner, and J. Melngailis, "Aperiodic Resistance Oscillations in Narrow Inversion Layers in Si," *Phys. Rev. Lett.* **55,** 2987–2990 (1985).
13. S. B. Kaplan and A. Hartstein, "Universal Conductance Fluctuations in Narrow Si Accumulation Layers," *Phys. Rev. Lett.* **56,** 2403–2406 (1986).
14. S. B. Kaplan and A. Hartstein, "Universal Conductance Fluctuations in Pinched-Channel Accumulation Layers," *Proceedings of the 18th International Conference on the Physics of Semiconductors*, World Scientific Press, Singapore, 1987, pp. 1499–1502.
15. W. J. Skocpol, P. M. Mankiewich, R. E. Howard, L. D. Jackel, D. M. Tennant, and A. Douglas Stone, "Universal Conductance Fluctuations in Silicon Inversion-Layer Nanostructures," *Phys. Rev. Lett.* **56,** 2865–2868 (1986).
16. A. Benoit, C. P. Umbach, R. B. Laibowitz, and R. A. Webb, "Length-Independent Voltage Fluctuations in Small Devices," *Phys. Rev. Lett.* **58,** 2343–2346 (1987).
17. W. J. Skocpol, P. M. Mankiewich, R. E. Howard, L. D. Jackel, D. M. Tennant, and A. D. Stone, "Nonlocal Potential Measurements of Quantum Conductors," *Phys. Rev. Lett.* **58,** 2347–2350 (1987).
18. A. D. Stone, "Magnetoresistance Fluctuations in Mesoscopic Wires and Rings," *Phys. Rev. Lett.* **54,** 2692–2695 (1985).
19. P. A. Lee and A. D. Stone, "Universal Fluctuations in Metals," *Phys. Rev. Lett.* **55,** 1622–1625 (1985).
20. B. L. Al'tshuler and D. E. Khmel'nitskiĭ, "Fluctuation Properties of Small Conductors," *Pis'ma Zh. Eskp. Teor. Fiz.* **42,** 291–293 (1985) [*JETP Lett.* **42,** 360–362 (1985)].
21. P. A. Lee, A. D. Stone, and H. Fukuyama, "Universal Conductance Fluctuations in Metals: Effects of Finite Temperature, Interactions, and Magnetic Field," *Phys. Rev. B* **35,** 1039–1070 (1987).
22. S. Feng, P. A. Lee, and A. D. Stone, *Phys. Rev. Lett.* **56,** 1960–1963 (1986); erratum, **56,** 2772 (1986).
23. Y. Isawa, H. Ebisawa, and S. Maekawa, "Theory of Aharonov–Bohm Effect in Small Normal Metals," *J. Phys. Soc. Jpn.* **55,** 2523–2526 (1986).
24. B. Doucot and R. Rammal, "Interference Effects and Magnetoresistance Oscillations in Normal-Metal Networks: I. Weak Localization Approach," *J. Phys. (Paris)* **47,** 973–999 (1986).
25. M. Büttiker, "Voltage Fluctuations in Small Conductors," *Phys. Rev. B* **35,** 4123–4126 (1987).
26. In a field-effect transistor, electrons (or holes) are confined near the surface of a semiconductor by an electric field. The electron layers induced by the field effect in n- and p-type field-effect transistors are called accumulation and inversion layers, respectively. See S. M. Sze, *Physics of Semiconductor Devices*, John Wiley & Sons, Inc., New York, 1981, Ch. 7.
27. Y. Aharonov and D. Bohm, "Significance of Electromagnetic Potentials in the Quantum Theory," *Phys. Rev.* **115,** 485–491 (1959); "Further Considerations on Electromagnetic Potentials in the Quantum Theory," *Phys. Rev.* **123,** 1511–1524 (1961).
28. R. Landauer, "Spatial Variation of Currents and Fields Due to Localized Scatterers in Metallic Conduction," *IBM J. Res. Develop.* **1,** 223–231 (1957).
29. R. Landauer, "Electrical Resistance of Disordered One-Dimensional Lattices," *Phil. Mag.* **21,** 863–867 (1970).
30. R. A. Webb, S. Washburn, C. P. Umbach, and R. B. Laibowitz, "Observation of h/e Aharonov–Bohm Oscillations in Normal-Metal Rings," *Phys. Rev. Lett.* **54,** 2696–2699 (1985).
31. The observation of low-field magnetoconductance oscillations with periodicity $h/2e$ in multiply-connected conductors is due to a different effect, and is beyond the scope of this paper.
32. A. B. Fowler, A. Hartstein, and R. A. Webb, "Conductance in Restricted-Dimensionality Accumulation Layers," *Phys. Rev. Lett.* **48,** 196–199 (1982).
33. P. A. Lee, "Variable-Range Hopping in Finite One-Dimensional Wires," *Phys. Rev. Lett.* **53,** 2042–2045 (1984).
34. M. Ya. Azbel, "Quantum d-Dimensional Landauer Formula," *J. Phys. C* **14,** L225–L232 (1981).
35. M. Büttiker, Y. Imry, R. Landauer, and S. Pinhas, "Generalized Many Channel Conductance Formula with Application to Small Rings," *Phys. Rev. B* **31,** 6207–6215 (1985).
36. A. D. Stone and Y. Imry, "Periodicity of the Aharonov–Bohm Effect in Normal-Metal Rings," *Phys. Rev. Lett.* **56,** 189–192 (1986).
37. B. L. Al'tshuler, A. G. Aronov, and D. E. Khmel'nitskiĭ, "Effect of Electron–Electron Collisions with Small Energy Transfers on Quantum Localization," *J. Phys. C* **15,** 7367–7386 (1982).
38. T. Ando, A. B. Fowler, and F. Stern, "Electronic Properties of Two-Dimensional Systems," *Rev. Mod. Phys.* **54,** 437–672 (1982).
39. K. Ishibashi, K. Nagata, K. Gamo, S. Namba, S. Ishida, K. Murase, and Y. Aoyagi, "Universal Magnetoconductance Fluctuations in Narrow n^+ GaAs Wires," *Solid State Commun.* **61,** 385–389 (1986).
40. R. P. Taylor, M. L. Leadbetter, G. P. Whittington, P. C. Main, L. Eaves, S. P. Beaumont, I. McIntyre, S. Thomas, and C. D. W. Wilkinson, "Universal Conductance Fluctuations in the Magnetoresistance of Submicron Size n^+ GaAs Wires and Laterally-Confined n^- GaAs/(AlGa)As Heterostructures," *Surf. Sci* **196,** 52–88 (1988).
41. E. Abrahams, P. W. Anderson, D. C. Liccardello, and T. V. Ramakrishnan, "Scaling Theory of Localization: Absence of Quantum Diffusion in Two Dimensions," *Phys. Rev. Lett.* **42,** 672–675 (1979).
42. B. L. Al'tshuler and A. G. Aronov, "Magnetoresistance of Thin Films and of Wires in a Longitudinal Magnetic Field," *Pis'ma Zh. Eskp. Teor. Fiz.* **33,** 515–518 (1981) [*JETP Lett.* **33,** 499–501 (1981)].
43. J. Mathews and R. L. Walker, *Mathematical Methods of Physics*, W. A. Benjamin Publishers, New York, 1970, pp. 383–384.
44. The explanation given in [12] made use of the concept of the thermal diffusion length $L_T \equiv \sqrt{hD/k_B T}$, which describes the distance over which thermal processes disturb the phase. L_T becomes smaller than L_ϕ when $k_B T$ exceeds E_ϕ.
45. S. Datta, M. R. Melloch, S. Bandyopadhyay, R. Noren, M. Vaziri, M. Miller, and R. Reifenberger, "Novel Interference

Effects Between Parallel Quantum Wells," *Phys. Rev. Lett.* **55,** 2344–2347 (1985).
46. G. Timp, A. M. Chang, P. deVegvar, R. E. Howard, R. Behringer, J. E. Cunningham, and P. Mankiewich, to be published in *Surf. Sci.*; G. Timp, A. M. Chang, J. E. Cunningham, T. Y. Chang, P. Mankiewich, R. Behringer, and R. E. Howard, "Observation of the Aharonov–Bohm Effect for $\omega_c\tau > 1$," *Phys. Rev. Lett.* **58,** 2814–2817 (1987).
47. M. L. Roukes, A. Scherer, S. J. Allen, Jr., H. G. Craighead, R. M. Ruthen, E. D. Beebe, and J. P. Harbison, "Quenching of the Hall Effect in a One-Dimensional Wire," *Phys. Rev. Lett.* **59,** 3011–3014 (1987).
48. J. A. Simmons, D. C. Tsui, and G. Weimann, "Quantum Interference Effects in High-Mobility Mesoscopic $GaAs/Al_xGa_{1-x}As$ Heterostructures," *Surf. Sci. 196,* 81–88 (1988).
49. R. Landauer, "Nonlinearity: Historical and Technical View," *Nonlinearity in Condensed Matter,* A. R. Bishop, D. K. Campbell, S. E. Trullinger, and P. Kumar, Eds., Springer-Verlag, Heidelberg, 1987, pp. 2–22.
50. S. B. Kaplan, "Structure in the Rectifying Behavior of Mesoscopic Si MOSFETs," *Surf. Sci.* **196,** 93–100 (1988); S. B. Kaplan, "Asymmetric Conductance and Coherence Effects in Mesoscopic Si MOSFETs," preprint; available from S. B. Kaplan, IBM Thomas J. Watson Research Center, P.O. Box 218, Yorktown Heights, NY 10598.
51. The formulas in [21] describing the effect of sample size on the fluctuation amplitudes depended somewhat on the shape of the sample, and were obtained using specific boundary conditions. The large device was expected to better conform to the boundary conditions and the limit $L, W \gg L_\phi$ described by theory.
52. Simply adding $G(V_{SD})$ and $G(-V_{SD})$ does not remove the contribution of asymmetric effects.
53. A. I. Larkin and D. E. Khmel'nitskiĭ, "Mesoscopic Fluctuations of Current–Voltage Characteristics," *Zh. Eksp. Teor. Fiz.* **91,** 1815–1817 (1986). [*Sov. Phys. JETP* **64,** 1075–1077 (1987)].
54. The constant of proportionality as discussed in [21] is shape-dependent, but not enough experimental work has been done to confirm these results. The shapes of these two devices are similar enough that this constant was assumed to be approximately the same for each sample.
55. R. A. Webb, A. Hartstein, J. J. Wainer, and A. B. Fowler, "Origin of the Peaked Structure in the Conductance of One-Dimensional Silicon Accumulation Layers," *Phys. Rev. Lett.* **54,** 1577–1580 (1985).
56. A. B. Fowler, G. L. Timp, J. J. Wainer, and R. A. Webb, "Observation of Resonant Tunneling in Silicon Inversion Layers," *Phys. Rev. Lett.* **57,** 138–141 (1986).
57. M. A. Kastner, R. F. Kwasnick, J. C. Licini, and D. J. Bishop, "Conductance Fluctuations Near the Localized-to-Extended Transition in Narrow Si Metal-Oxide-Semiconductor Field-Effect Transistors," *Phys. Rev. B* **36,** 8015–8031 (1987).

Received November 3, 1987; accepted for publication December 15 1987

Steven B. Kaplan *IBM Thomas J. Watson Research Center, P.O. Box 218, Yorktown Heights, New York 10598.* Dr. Kaplan is a Research Staff Member in the Inversion Layers Group, where he has studied low-temperature quantum transport and electronic interference effects. He joined IBM in 1979 at the Thomas J. Watson Research Center, working on various aspects of digital Josephson technology. Dr. Kaplan's postdoctoral fellowship at the National Bureau of Standards in Boulder, Colorado, and his Ph.D. work at the University of Pennyslvania were spent on the study of nonequilibrium superconductivity.

Allan M. Hartstein *IBM Thomas J. Watson Research Center, P.O. Box 218, Yorktown Heights, New York 10598.* Dr. Hartstein is manager of the Inversion Layers Project at the Thomas J. Watson Research Center. He received a B.S. degree in physics from the California Institute of Technology in 1969 and a Ph.D. degree in physics from the University of Pennsylvania in 1973. Dr. Hartstein joined IBM at the Thomas J. Watson Research Center in 1974. His research activities have focused on the study of 1D and 2D transport properties in silicon MOSFETs; he has also studied electron tunneling phenomena and infrared absorption from molecular monolayers. Dr. Hartstein is a Fellow of the American Physical Society.